A&A manuscript no.
(will be inserted by hand later)

Your thesaurus codes are:
03(02.01.2; 02.02.1; 11.01.2; 02.18.7)

ASTRONOMY
AND
ASTROPHYSICS
6.12.1995

Vertical Structure and Spectrum of Accretion Disks in Active Galactic Nuclei

T. Dörrer[1], H. Riffert[2], R. Staubert[1], and H. Ruder[2]

[1] Institut für Astronomie und Astrophysik, Astronomie, Universität Tübingen, Waldhäuserstr. 64, D-72076 Tübingen, Germany
[2] Institut für Astronomie und Astrophysik, Theoretische Astrophysik, Universität Tübingen, Auf der Morgenstelle 10, D-72076 Tübingen, Germany

Received date; accepted date

Abstract. Radiation emitted from an accretion disk around a massive black hole is a widely discussed model for the UV/soft X–ray excess emission observed in the spectra of many AGN. A self–consistent calculation of the structure and the emerging spectrum of geometrically thin α–accretion disks in AGN is presented. The central object is assumed to be a Kerr black hole; full relativistic corrections are included. The local dissipation of gravitational energy is assumed to be entirely due to turbulence. Since these disks are mainly supported by radiation pressure, the assumption that the viscous energy production is proportional to the total pressure leads to diverging temperature structures in the upper parts of the disk, where the total optical depths is small. We therefore modify the standard expression for the turbulent viscosity by taking into account the radiative energy loss of turbulent elements in an optically thin regime. Compton scattering is treated in the Fokker–Planck approximation using the Kompaneets oparator. The absorption cross section contains only free–free processes for a pure hydrogen atmosphere. We present several calculations for various parameters such as the accretion rate $\dot{M}$, the viscosity parameter α, the specific angular momentum a of the black hole and the inclination angle Θ_0 of the observer. The resulting temperature and density profiles show that the disks are optically thick for Compton scattering and effectively optically thin for most frequencies. This leads to spectra that are diluted with respect to the photon number but contain a Comptonized high energy tail in order to carry the required energy flux. In addition the electron temperature deviates strongly from the equilibrium temperature. For a model with $M = 10^8 M_\odot$, $\dot{M} = 0.3$, $\alpha = 1/3$ and $a/M = 0.998$ the fraction of total flux emitted in the soft and hard X–ray band ($> 2.4 \cdot 10^{16} Hz$) for $\Theta_0 = 0°, 41°, 60°, 70°$ and $90°$ is 36%, 50%, 64%, 78% and 93%, respectively. Therefore, the model can in general account for the observed soft X–ray excess.

Key words: accretion disks – black hole physics – Galaxies: active – radiative transfer

Send offprint requests to: R. Staubert

1. Introduction

Dissipation of gravitational energy by accretion onto a massive black hole is regarded as the origin of the enormous luminosities of active galactic nuclei (AGN). Since the accreted matter is likely to carry some angular momentum, it is common to invoke the presence of an accretion disk. A strong observational evidence for such disks comes from the spectral flattening in the optical/UV seen in many AGN, the so–called "big blue bump" (e. g. Shields 1978; Malkan & Sargent 1982). This spectral feature is thought to be due to thermal emission from an accretion disk and perhaps extends into the soft X–ray band, producing a steep excess emission known as the "soft excess" (e. g. Arnaud et al. 1985; Wilkes & Elvis 1987; Turner & Pounds 1989). Other evidence comes from the reflection hump and iron emission line observed in AGN (e. g. Pounds et al. 1990).

The standard theory of thin accretion disks is largely based on the fundamental papers of Shakura & Sunyaev (1973, hereafter SS73) and Novikov & Thorne (1973, hereafter NT73). The simplest way to calculate the emitted disk spectrum is to assume that the disk is geometrically thin but optically thick and radiates locally as a blackbody. The effective temperature $T_{\rm eff}$ of the blackbody is then solely determined by the dissipated flux per unit area. These simple disk models, however, are not able to produce soft X–rays as long as they do not become super–Eddington (e. g. Bechtold et al. 1987). Real disk spectra will differ from the blackbody approximation: for sufficiently high accretion rates and viscosity parameters, the accretion disk eventually becomes effectively optically thin at small radii and the gas temperature strongly deviates from the equilibrium temperature in such cases. Even in the optically thick case the local spectra differ from the blackbody, because the scattering opacity dominates over absorption in the soft X–ray regime and there exists a temperature gradient in the vertical direction.

In the last few years several calculations of increasing accuracy have been performed to determine the structure and emission spectrum of accretion disks around massive black holes. Contrary to the standard Newtonian disk model, NT73 and Page & Thorne (1974) calculated the effects of general relativity on the disk structure. The propagation of photons from the disk surface to a distant observer was treated by Cunningham (1975). On the other hand, SS73, Czerny & Elvis (1987), and Wandel & Petrosian (1988) concentrated on a proper calculation of the radiative transfer by discussing the effects of Comptonization in a simple analytic manner. Laor & Netzer (1989) and Laor et al. (1990) included relativistic effects as well as free–free and bound–free opacities in their numerical computations. Most calculations of model spectra to date, however, made use of an averaging over the vertical direction. Ross, Fabian & Mineshige (1992, hereafter RFM) have calculated the vertical temperature profile and atomic level populations in the radiation pressure dominated inner regions of the disk for a given constant vertical density profile, using the Kompaneets equation to treat Compton scattering. Relativistic corrections for a non–rotating black hole were incorporated in this code by Yamada et al. (1994). Shimura & Takahara (1993) and Shimura & Takahara (1995) have calculated the vertical structure and radiation field of a Newtonian disk self–consistently, using the ad hoc assumption that the local viscous heating rate is proportional to the mass density ρ.

Here we have also calculated the z–structure simultaneously with the radiation field of the disk. But we use a different viscosity description. We assume that the local energy production is caused by turbulence. The standard α–description (viscosity proportional to the total pressure) leads to diverging temperature profiles in the upper optically thin regions of the disk, because viscous heating always exceeds radiative cooling. We therefore propose a modification of the standard α–model, which includes the radiative cooling of the turbulent elements. The frequency dependent radiative transfer equation is solved in the Eddington approximation and the effects of Compton scattering are treated by the Kompaneets equation (Kompaneets 1957). Relativistic corrections on the local disk structure are introduced according to Riffert & Herold (1995) for rotating and non–rotating black holes. In this paper we present solutions of the local structure and the emission spectrum of accretion disks for different input parameters (accretion rate, viscosity parameter). Integrated disk spectra, as seen from a distant observer, are calculated by the use of a transfer function (e. g. Cunningham 1975; Speith et al. 1995). In Sect. 2 the basic equations and viscosity description of our model are formulated. In Sect. 3 numerical results are presented. Finally, our results and conclusions are summarized in Sect. 4.

2. The Model

2.1. Basic Equations

We adopt the standard geometrically thin α–accretion disk model, i.e. the disk height H is much smaller than the radius r, and the dominant velocity is given by the Keplerian motion around the central mass. The disk is assumed to be in a stationary and rotationally symmetric state, thus all functions depend only on the radial and vertical coordinates r and z. The relativistic disk structure has been calculated by NT73 and subsequently by Riffert & Herold (1995), correcting a term in the vertical pressure balance. According to this paper we define four relativistic correction factors with respect to the standard Newtonian disk model depending on the mass M and the specific angular momentum a/M of the central black hole:

$$
\begin{aligned}
A &= 1 - \frac{2GM}{c^2 r} + \frac{a^2}{c^2 r^2} \\
B &= 1 - \frac{3GM}{c^2 r} + \frac{2a\sqrt{GM}}{c^2 r^{3/2}} \\
C &= 1 - \frac{4a\sqrt{GM}}{c^2 r^{3/2}} + \frac{3a^2}{c^2 r^2} \\
D &= \frac{1}{2\sqrt{r}} \int_{r_i}^{r} \frac{x^2c^2 - 6xGM + 8a\sqrt{xGM} - 3a^2}{\sqrt{x}\left(x^2c^2 - 3xGM + 2a\sqrt{xGM}\right)}\, dx \quad . \qquad (1)
\end{aligned}
$$

r_i is the inner disk radius located at the position of the last stable circular orbit; the gravitational constant and the velocity of light are denoted by G and c.

The hydrostatic equilibrium in vertical direction for a thin accretion disk is given by

$$
\frac{dP}{dz} = -\rho g_z = -\rho \frac{GM}{r^3} z \frac{C}{B} \, , \qquad (2)
$$

where P, ρ, and g_z are the total pressure, the mass density, and the gravitational acceleration, respectively.

The radiative transfer is solved in the Eddington approximation, and Compton scattering is treated in the Fokker–Planck approximation using the Kompaneets operator. The absorption cross section contains only free–free processes for a pure hydrogen atmosphere. Induced contributions to the radiative processes have been neglected throughout.

Assuming the plasma to be in a state of local thermodynamic equilibrium (LTE) the first two moments of the radiative transfer equation for the spectral energy density U_ν and the spectral flux F_ν read

$$
\frac{\partial F_\nu}{\partial z} = \kappa_\nu^{\rm ff} \rho c [W_\nu - U_\nu] + \kappa_T \rho \frac{8\pi h^2}{m_e c^4} \nu \frac{\partial}{\partial \nu} \nu^4 \left[n_\nu + \frac{kT}{h} \frac{\partial n_\nu}{\partial \nu} \right] \qquad (3)
$$

$$
\frac{1}{3} \frac{\partial U_\nu}{\partial z} = -\frac{\rho}{c} [\kappa_T + \kappa_\nu^{\rm ff}] F_\nu \, . \qquad (4)
$$

Here $W_\nu = 8\pi h \nu^3 c^{-3} \exp(-h\nu/kT)$ is the Wien function which serves as the equilibrium spectrum in this case, $\kappa_\nu^{\rm ff}$ is the free–free opacity, and $\kappa_T = 0.4\ {\rm g/cm^2}$ is the Thomson opacity. The photon occupation number n_ν can be expressed in terms of U_ν

$$
n_\nu = \frac{c^3}{8\pi h \nu^3} U_\nu \, . \qquad (5)
$$

The free–free opacity is given by

$$
\kappa_\nu^{\rm ff} = 1.3 \cdot 10^{56} \rho T^{-1/2} \nu^{-3} \bar{g}_{\rm ff}\, cm^2\, g^{-1} \, , \qquad (6)
$$

where T is the gas temperature, k is the Boltzmann constant, and $\bar{g}_{\rm ff}$ is the thermal average free–free Gaunt factor (Karzas & Latter 1961; Carson 1988).

In the Eddington approximation the equation of state can be written as

$$P = P_{gas} + P_{rad} = \frac{k}{\mu m_u}\rho T + \frac{1}{3}U \ , \tag{7}$$

where $U = \int_0^\infty U_\nu \, d\nu$ is the total energy density of the radiation field, m_u is the atomic mass unit and μ is the mean molecular weight with $\mu = 1/2$ for a fully ionized hydrogen atmosphere.

For a Keplerian disk, the viscous heating rate per unit volume $\dot{Q}_{visc}$ is related to the ϕ–r–component of the viscous stress tensor $\mathbf{t}$ by

$$\dot{Q}_{visc} = \frac{3}{2}\sqrt{\frac{GM}{r^3}} t_{\phi r} \frac{A}{B} \ , \tag{8}$$

and $t_{\phi r}$ can be expressed in terms of velocity gradients leading to the result

$$t_{\phi r} = \frac{3}{2}\eta\sqrt{\frac{GM}{r^3}}\frac{A}{B} \ , \tag{9}$$

with the shear viscosity η.

In a steady state this heating rate must be balanced by the total radiative cooling, since convection is not considered in this model. Integration of the right–hand side of equation (3) over frequency ν leads to the following energy balance equation

$$\dot{Q}_{visc} = \frac{dF}{dz} = \int_0^\infty \frac{\partial F_\nu}{\partial z} \, d\nu \ . \tag{10}$$

The disk model is so far described by the equations (2), (3), (4), (7) and (10) which can be solved numerically when proper boundary conditions are imposed. The only unspecified process is the source of viscosity and this will be discussed in the next section.

Because of symmetry reasons the inner boundary condition in the midplane of the disk ($z = 0$) is taken as

$$F_\nu(z = 0) = 0 \ , \tag{11}$$

and at the upper boundary (at $z = H$) we assume that the disk radiates isotropically into the vacuum

$$F_\nu = \frac{c}{2}U_\nu \ . \tag{12}$$

For a geometrically thin accretion disk the energy flux from the disk surface ($z = H$) is

$$F(z = H) = \int_0^\infty F_\nu \, d\nu = \frac{3GM\dot{M}}{8\pi r^3}\frac{D}{B} \ , \tag{13}$$

where $\dot{M}$ is the total mass flux through the disk.

Finally, the disk height H is specified by the condition

$$\rho(z = H) = 0 \tag{14}$$

We solve the above set of equations for the functions ρ, T, H, U_ν, and F_ν using a finite difference scheme in both variables z and ν. The vertical structure is resolved with 100 points on a logarithmic grid, and 64 grid points are used in frequency space. The resulting set of algebraic difference equations is then solved by a Newton–Raphson method.

Once the vertical structure has been determined we can integrate the density profiles to obtain the surface density $\Sigma(r) = \int_{-H}^{+H} \rho(z) \, dz$ and the average radial velocity $|v_r| = \dot{M}/\Sigma(r)$. In order to justify the basic assumptions of the thin disk model one must have $|v_r| \ll |v_\phi|$, where v_ϕ is the Keplerian velocity.

2.2. *The Viscosity Description*

In the standard α-model (SS73) the viscous stress tensor component $t_{\phi r}$ is propotional to the pressure

$$t_{\phi r} = \alpha P \ . \tag{15}$$

This is a consequence of a number of assumptions: first, the viscosity is caused by turbulence in the disk, and the magnitude of η can be estimated from a dimensional analysis

$$\eta \approx \rho \, l_{turb} V_{turb} \ , \tag{16}$$

where l_{turb} and V_{turb} are the size and the typical velocity of the largest turbulent eddies, respectively. Next, the disk height H is used for l_{turb} which is obtained from the hydrostatic equation (2)

$$H \approx \sqrt{\frac{B\, r^3}{C\, GM}}\sqrt{\frac{P_c}{\bar{\rho}}} \ , \tag{17}$$

where P_c is the pressure in the midplane, and $\bar{\rho}$ stands for the average density. The turbulent velocity V_{turb} is assumed to be limited by the local sound speed c_s. Otherwise shocks would develop and heat the gas until the tubulence is subsonic. Approximating the ratio $P_c/\bar{\rho}$ by the local value $P/\rho = c_s^2$ and inserting the above relations into equation (9) for the viscous shear leads to the expression (15), where the constant α takes up all uncertainties in terms of numerical factors. This entire procedure is quite successful for the standard disks in cataclysmic variables which are dominated by the gas pressure. If radiation pressure becomes important a number of difficulties arise when the model is applied without modifications. According to equation (3) the radiative cooling decreases in the upper layers of the disk where the density drops exponentially. Since the radiation pressure remains finite in this region, the total heating rate (8) cannot be balanced by radiative losses. This could be cured by replacing P in equation (15) by the gas pressure, however, in an optically thick regime the radiation behaves like a gas exchanging momentum with the plasma and thus contributes to the viscous shear. In addition, in a radiation dominated disk gravity is mainly balanced by radiative forces and the disk height is then given by

$$H \approx \frac{3\dot{M}\kappa_F}{8\pi c}\frac{D}{C} \ , \tag{18}$$

where κ_F is a flux weighted average opacity

$$\frac{1}{\kappa_F} = \frac{\int_0^\infty \frac{1}{\kappa_T + \kappa_{\rm ff}} \frac{dU_\nu}{dz} \, d\nu}{\int_0^\infty \frac{dU_\nu}{dz} \, d\nu} \, . \tag{19}$$

This height does not contain the sound speed. In order to derive a consistent parameterization of the turbulent viscosity for the radiation dominated case we start from the dimensional analysis (16) using again $l_{turb} = H$, where the disk height H is self–consistently calculated in our model. For the limitation of the velocity V_{turb} the same arguments as in SS73 are used, i.e. V_{turb} has to be small enough that no entropy due to shock waves is generated in the flow. For a radiation dominated shock in an optically thick medium

$$V_{turb} < \sqrt{\frac{P}{\rho}} \, , \tag{20}$$

but in an optically thin regime, where the photons are able to escape freely

$$V_{turb} < \sqrt{\frac{P_{gas}}{\rho}} \, . \tag{21}$$

This follows from considering an isothermal shock in a plasma with radiation when the Mach number approaches unity. Assuming an isothermal shock structure is an approximation for an optically thin environment. Since this limiting value of V_{turb} depends on the optical depth we interpolate between the two extreme cases

$$V_{turb} = c_s \frac{\tau + \sqrt{\beta}}{1 + \tau} \, , \tag{22}$$

with the optical depth

$$\tau = \int_z^H \kappa_F \rho \, dz' \, , \tag{23}$$

and the pressure ratio $\beta = P_{gas}/P$. For the turbulent viscosity we now have

$$\eta = \alpha \rho H V_{turb} \, , \tag{24}$$

with a constant α which is a parameter in our disk model.

We will now consider the heating–cooling balance, integrate equation (3) over frequency, and use the relations (10) and (8)

$$\begin{aligned} \frac{dF}{dz} &= \bar{\kappa}_{\rm ff} \rho c \left[a_r T^4 - U \right] + 4U \frac{\kappa_T \rho}{m_e c} \left[kT - <\nu> \right] \\ &= \frac{9GM}{4r^3} \frac{A^2}{B^2} \alpha \rho H V_{turb} \, , \end{aligned} \tag{25}$$

where $\bar{\kappa}_{\rm ff}$ is some appropriately averaged mean absorption opacity, a_r is the radiation constant, and

$$<\nu> = \frac{\int_0^\infty \nu^4 n_\nu \, d\nu}{4 \int_0^\infty \nu^3 n_\nu \, d\nu} \tag{26}$$

is an average photon energy ($h <\nu> /k = T_r$ can be considered as a radiation temperature). In the upper parts of the disk (at $z \approx H$) the density drops to zero and since $\bar{\kappa}_{\rm ff} \propto \rho$ free–free processes are negligible in this regime. The radiation field remains unchanged and thus $<\nu>$ and U are constant; from the boundary condition $c\,U(H) = 2\,F(H)$ we obtain using equations (13), (18), and (22) for $\tau \ll 1$

$$T - T_r = \sqrt{T_v T} \, , \tag{27}$$

where

$$T_v = \left(\frac{9\alpha}{32}\right)^2 \left(\frac{\kappa_F}{\kappa_T}\right)^2 \frac{m_e^2 c^2}{\mu k m_u} = 5.1\,10^5\,\alpha^2 \left(\frac{\kappa_F}{\kappa_T}\right)^2 \ {\rm K} \, . \tag{28}$$

(Note that in a scattering dominated plasma $\kappa_F/\kappa_T \approx 1$). From this we get the temperature that will result from a balance of viscous heating and inverse Compton cooling

$$T = T_r + \frac{1}{2} \left[T_v + \sqrt{T_v^2 + 4 T_r T_v} \right] \, . \tag{29}$$

This solution is unique since a negative sign of the square root in (29) would correspond to a negative sign of the right hand side of equation (27). As a consequence we obtain a lower limit for T

$$T > max[T_r, T_v] \, . \tag{30}$$

3. Results

In this paper the mass of the black hole is fixed at a typical value of $M = 10^8 M_\odot$. We show results of our model calculations for different input parameters such as the accretion rate $\dot{M}$, the viscosity parameter α, the specific angular momentum a, and the inclination angle Θ_0 of the observer's position with respect to the disk axis. Hereafter, $\dot{M}$ is measured in units of the critical accretion rate $\dot{M}_{crit} = L_{Edd}/(\varepsilon c^2)$, where $L_{Edd} = 4\pi c G M/\kappa_T$ is the Eddington luminosity and ε is the efficiency of accretion. For a non–rotating black hole ($a/M = 0$) ε is 0.057, and for a maximally rotating black hole ($a/M \simeq 0.998$, see Thorne 1974) $\varepsilon \simeq 0.321$. First, we give solutions of the local vertical structure and emission spectrum at 5 Schwarzschild radii ($r = 5R_S = 10GM/c^2$). At this radius, the local energy release takes its maximum value for a non–rotating black hole and this disk region is responsible for the high frequency part of the total spectrum. Next, we consider the radial structure and the integrated disk spectrum seen by a distant observer. At this point we also include relativistic effects on the emergent disk spectrum such as the relativistic Doppler shift from the disk rotation, gravitational redshift, and gravitational light bending due to the central black hole.

3.1. Vertical Structure and Local Disk Spectrum

A typical vertical distribution (normalized to the corresponding maximum values) of the radiative flux F, the radiation energy density u, the mass density ρ, and the gas temperature T as a function of the Thomson scattering optical depth τ_T is shown in Fig. 1 for a non–rotating black hole with $M = 10^8 M_\odot$, $\dot{M} = 0.3$, $\alpha = 1/3$ and $r = 5R_S$. In Fig. 2, the above variables are plotted for the case of a maximally rotating black hole ($a/M = 0.998$) with the same input parameters, but using $r = 1R_S$, which nearly corresponds to the maximum of the local energy release for $a/M = 0.998$. It is found that the mass

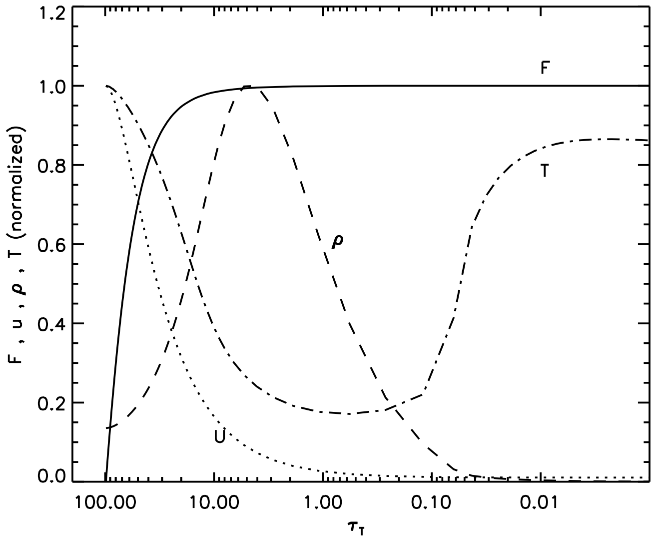

Fig. 1. Vertical distribution of radiative flux F, radiation energy density U, mass density ρ, and gas temperature T (all normalized to their respective maximum values) at $r = 5R_S$. The model parameters are: $M = 10^8 M_\odot$, $\dot{M} = 0.3$, $\alpha = 1/3$, $a/M = 0$. Note that U approaches a finite value for small optical depth ($\tau_T \to 0$).

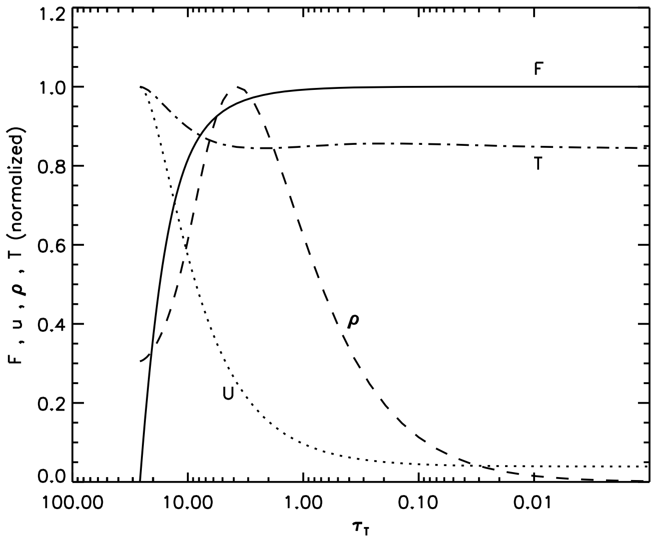

Fig. 2. Same as Fig. 1, but for a maximally rotating black hole $a/M = 0.998$ at $r = 1R_S$.

density ρ is not a monotonically decreasing function of z, but is showing a clear density inversion (such density inversions have also been found by Meyer & Meyer–Hofmeister 1982 and Milsom et al. 1994). This can be explained as follows: in using the flux weighted mean κ_F (equation (19)), the hydrostatic equilibrium can be written as

$$\frac{dP_{gas}}{dz} = \frac{\kappa_F}{c}\rho[(F(z) - F_{Edd}(z)] = -\rho g_z^* \,, \tag{31}$$

where the local Eddington flux $F_{Edd}(z)$ is given by

$$F_{Edd}(z) = \frac{c}{\kappa_F} g_z \,, \tag{32}$$

and $g_z^* = g_z - \kappa_F F/c$ is the effective gravitational acceleration. For a highly radiation pressure dominated disk ($P_{rad} \gg P_{gas}$), the local flux adjusts itself close to the Eddington value. For example, the radiation pressure always exceeds the gas pressure by at least a factor of about 100 throughout the disk for the parameters adopted in Fig. 1. When the emerging surface flux is large, the local flux becomes slightly super–Eddington in the inner regions of the disk and a strong density inversion ($d\rho/dz > 0$) occurs. Because of the boundary condition imposed on the surface flux, the outer parts of the disk are always sub–Eddington. In Fig. 3 the vertical density distribution is shown for different $\dot{M}$. The density in the equatorial plane is up to a factor of 7 smaller than its maximum value. Although

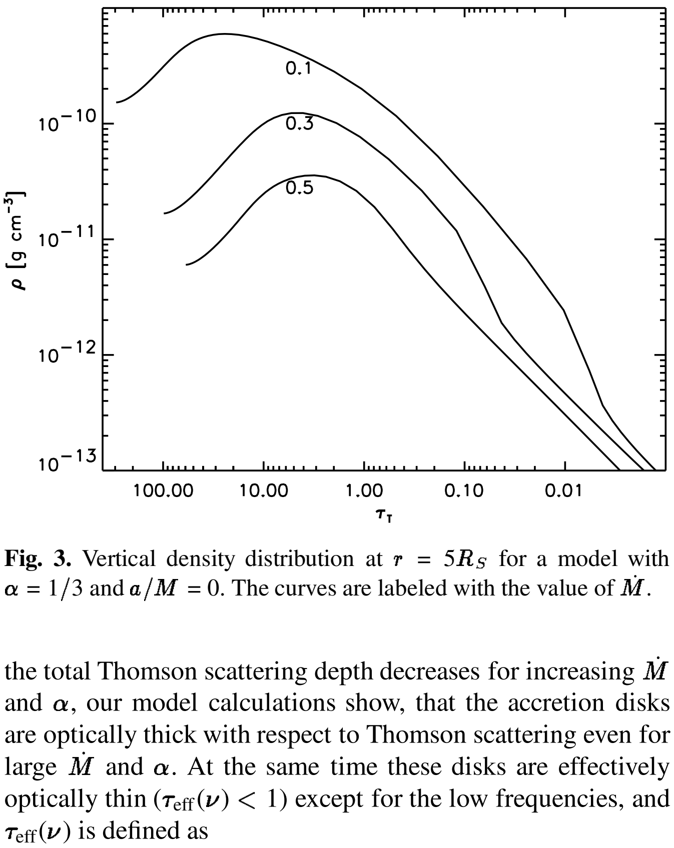

Fig. 3. Vertical density distribution at $r = 5R_S$ for a model with $\alpha = 1/3$ and $a/M = 0$. The curves are labeled with the value of $\dot{M}$.

the total Thomson scattering depth decreases for increasing $\dot{M}$ and α, our model calculations show, that the accretion disks are optically thick with respect to Thomson scattering even for large $\dot{M}$ and α. At the same time these disks are effectively optically thin ($\tau_{\rm eff}(\nu) < 1$) except for the low frequencies, and $\tau_{\rm eff}(\nu)$ is defined as

$$\tau_{\rm eff}(\nu) = \int_0^H \rho\sqrt{3 \cdot [\kappa_{\rm ff}(\nu) + \kappa_T]\kappa_{\rm ff}(\nu)}\, dz \,. \tag{33}$$

In this case the assumption of local thermodynamic equilibrium (LTE) is no longer valid even in the disk midplane and the gas temperature deviates strongly from the equilibrium temperature defined as $T_{eq} = (U/a_r)^{1/4}$. The various heating and cooling functions are compared in Fig. 4. Compton cooling plays the

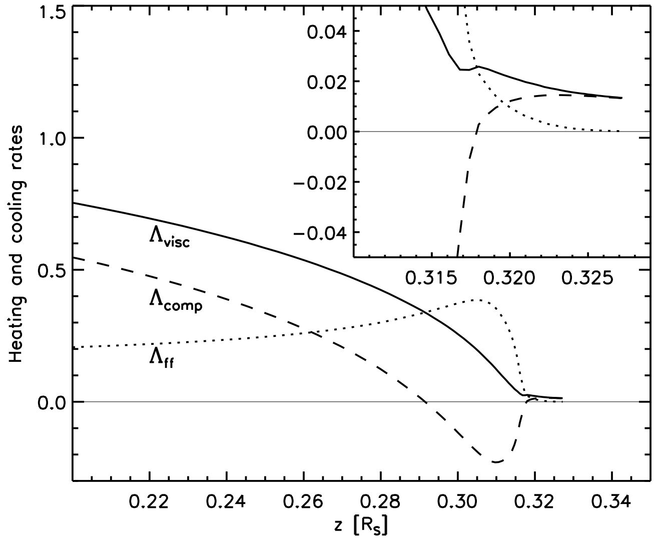

Fig. 4. Viscous heating Λ_{visc}, Compton cooling Λ_{comp} and cooling due to free–free emission Λ_{ff} (all normalized to the viscous heating rate at the disk midplane) as a function of z at $r = 5R_S$. The model parameters are: $M = 10^8 M_\odot$, $\dot{M} = 0.3$, $\alpha = 1/3$, $a/M = 0$. The outermost layer is shown in the upper right corner with higher resolution.

dominat role in the inner layers of the disk (at small z), whereas in the region of the density increase free-free-processes become very efficient leading to a steep temperature drop. The gas temperature even falls below the radiation temperature T_r, thus Compton scattering turns into a heating mechanism (Λ_{comp} is negative) which effectively balances the bremsstrahlung cooling. In the uppermost layers, where the density drops exponentially, free-free processes are negligible ($\propto \rho^2$), and the temperature adjusts itself to the equilibrium between viscous heating and inverse Compton cooling described above. Due to these heating-cooling processes a temperature inversion occurs and a hot corona-like layer builds up on top of the disk. This layer is however optically thin to both scattering and absorption (the typical densities are below $10^{-13}\,\mathrm{g\,cm^{-3}}$), and thus there is no effect on the emitted spectrum. Note that in the upper disk layers the viscous heating is proportional to the density, thus the relevant cooling mechanisms must not have a stronger ρ–dependence. This holds of course for inverse Compton cooling used in our model, however, cooling due to strong resonance lines has also been proposed (Hubeny 1990) to contribute to the overall heating–cooling balance.

The gas temperature and the corresponding equilibrium temperature T_{eq} for different $\dot{M}$ are shown in Fig. 5.

For large values of $\dot{M}$ even the temperature in the midplane of the disk strongly exceeds the equilibrium value. For low

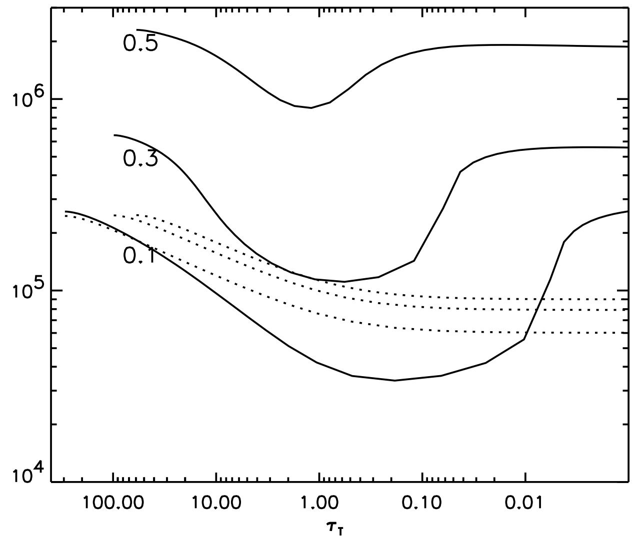

Fig. 5. Vertical distribution of gas temperature T (solid lines) and equilibrium temperature T_{eq} (dotted lines) at $r = 5R_S$ for a model with $\alpha = 1/3$ and $a/M = 0$. The curves are labeled with the value of $\dot{M}$.

$\dot{M}$ the disk becomes effectively optically thick and a general equilibrium is established.

The locally emitted spectrum at a fixed radial position ($r = 5R_S$) for different $\dot{M}$ is shown in Fig. 6. The local Wien

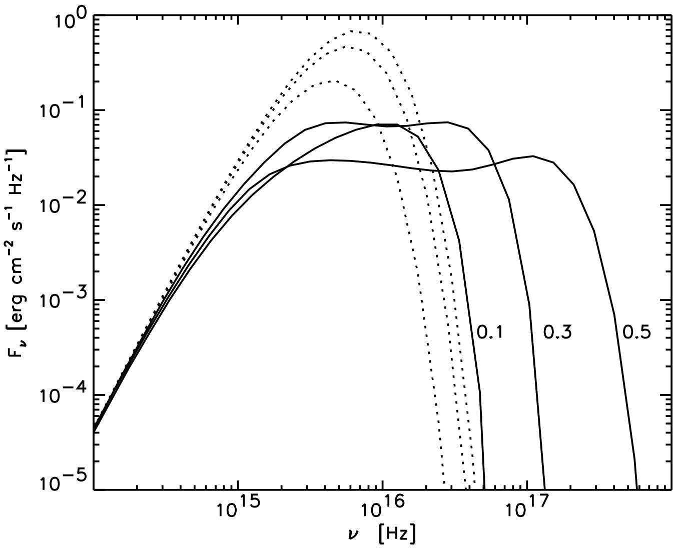

Fig. 6. Emergent spectrum at $r = 5R_S$ for $\alpha = 1/3$ and $a/M = 0$. The curves are labeled with the value of $\dot{M}$. Dotted curves show the local Wien spectrum at $T = T_{\rm eff}$.

spectra at the corresponding effective temperature $T_{\rm eff}$ are also shown by dotted lines. At low frequencies, the accretion disk is effectively optically thick and scattering effects can be neglected; the local spectrum approaches the equilibrium distribution W_ν, however, the spectra in low frequency regime cannot be taken too seriously since we have neglected induced processes. At higher frequencies, scattering effects become important and one gets a modified Wien spectrum. For sufficiently high $\dot{M}$ and α a Wien peak appears in the soft X–ray range of the local spectra. This feature is a result of repeated Compton scattering of photons by a thermal distribution of electrons at temperature T. If the Compton parameter $y \gg 1$, Comptonization goes to saturation and the photons are shifted into a Wien distribution at temperature T (see Felten & Rees 1972). The Compton parameter y is defined as

$$y = \frac{4kT}{m_e c^2}\tau_T^2 \, . \tag{34}$$

For example, the case $\dot{M} = 0.3$ shown in Fig. 6 leads to a effective optical depth $\tau_{\rm eff}(\nu_{max}) = 0.1$ at the peak frequency $\nu_{max} = 2.8 \cdot 10^{16}\,Hz$ and a total Thomson scattering depth of $\tau_T = 98.5$; from that and an average temperature of $T = 4 \cdot 10^5 K$ (see Fig. 5) we have $y \approx 3$. Since repeated Compton scattering is important for $y > 1$, a significant shift of photons into the Wien peak is expected. For low $\dot{M}$ and α the disk is effectively optically thick for all relevant frequencies and the radiation assumes an equilibrium spectrum for almost all z. The effective optical depth for the curve $\dot{M} = 0.1$ in Fig. 5 and 6 is $\tau_{\rm eff}(\nu_{max}) = 9.8$, with $\nu_{max} = 9.1 \cdot 10^{15}\,Hz$. Nevertheless, the emergent spectrum deviates from the Wien spectrum at $T = T_{\rm eff}$ because there exists a temperature gradient and high frequency photons escape from deeper layers with higher temperatures.

3.2. Radial Structure and Integrated Disk Spectrum

After discussion of the vertical structure and local emission spectrum at $r = 5R_S$ here we investigate the radial structure and overall spectrum of the accretion disk. In numerical calculations, we used 50 radial points on a logarithmic grid from the last stable orbit r_i to the outer disk radius r_{out} (here $r_{out} = 1000R_S$). The height of the disk from the surface to the equatorial plane as a function of the radial distance from the black hole is shown in Fig. 7 for several values of $\dot{M}$. For comparison, the geometrically thin limit, here defined as $H(r) = 0.1r$, is also plotted as a dashed curve. This means that the accretion rate should not greatly exceed $\dot{M} = 0.3$ for not to violate the geometrically thin disk approximation. Therefore, numerical results for higher accretion rates are strictly speaking not self–consistent. On the other hand, the α–parameter has little influence (of the order of a few per cent) on the height of the disk. If the local flux is given by the Eddington flux, the disk height H is given by equation (18). In the inner regions of the disk Thomson scattering delivers the major contribution to the opacity ($\kappa_F \approx \kappa_T$) and the height of the disk is solely determined by the accretion rate $\dot{M}$. However, the local flux deviates from the Eddington flux at the upper boundary of the disk. Although the gas pressure is negligible in comparison with the radiation pressure, the gas pressure gradient dp_{Gas}/dz is not. We have also determined mean radial velocities $|v_r| = \dot{M}/\Sigma(r)$ for all radial grid points. Our calculations show, that for $\dot{M} \leq 0.3$ and $\alpha \leq 1$ the basic thin disk approximation $|v_r| \ll |v_\phi|$ is always satisfied. Now we will turn to the integrated disk spectra. General relativistic effects on the emergent spectrum are twofold: first, relativistic effects occur in calculating the disk structure and therefore change the local emission spectrum in the corotating frame of the disk. The resulting spectra were discussed for a non–rotating black hole in section 3.1. Second, relativistic effects have a substantial influence on the propagation of photons to the observer. All these effects become more and more important if the black hole is rotating, since then the disk extends to regions very near to the black hole. To separate

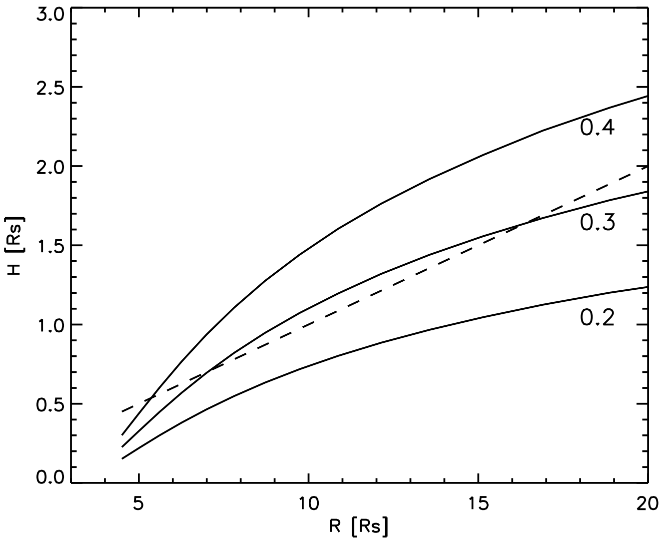

Fig. 7. Disk height for $\alpha = 1/3$ and $a/M = 0$. The curves are labeled with the value of $\dot{M}$. The dashed curve shows the geometrically thin limit $H(r) = 0.1 \cdot r$.

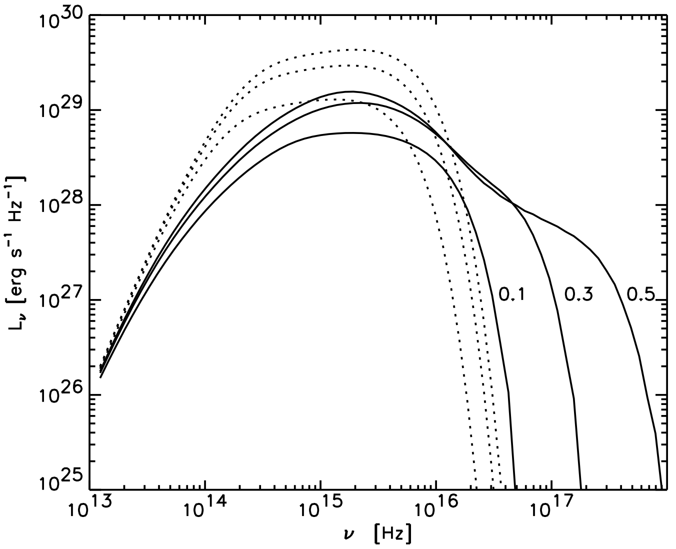

Fig. 8. Entire Newtonian face on disk spectra for $\alpha = 1/3$ and $a/M = 0$. The curves are labeled with the value of $\dot{M}$. Dotted curves denote multi Wien spectra.

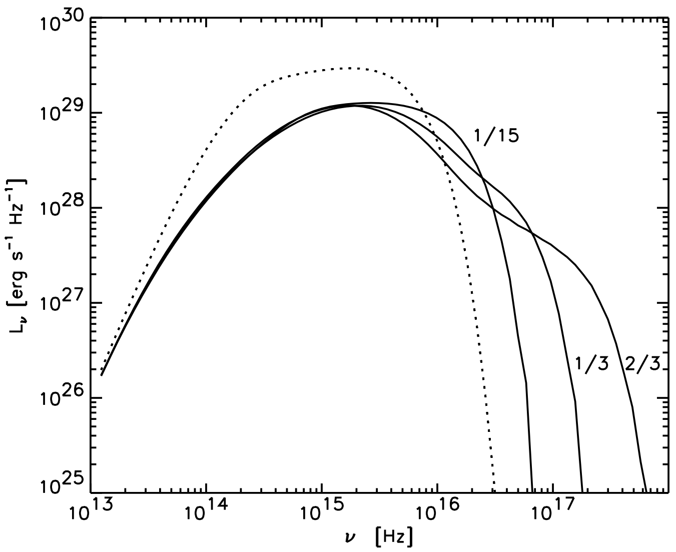

Fig. 9. Entire Newtonian face on disk spectra for $\dot{M} = 0.3$ and $a/M = 0$. The curves are labeled with the value of α. The dotted curve denotes the corresponding multi Wien spectrum.

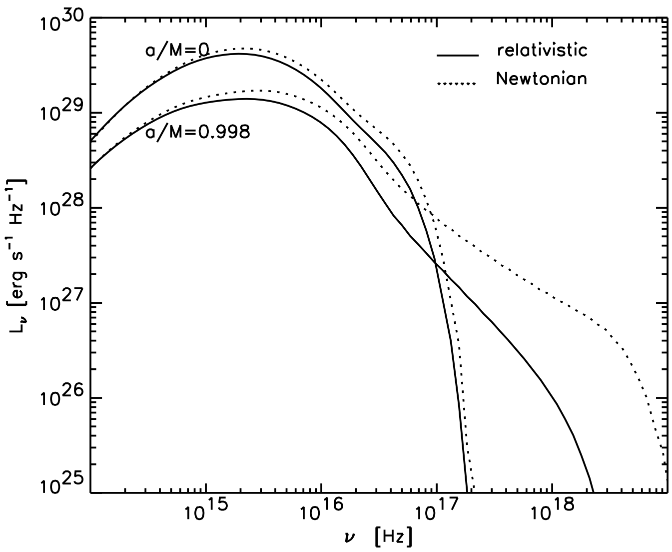

Fig. 10. Entire face on disk spectra for $\dot{M} = 0.3$ and $\alpha = 1/3$. The curves are labeled with the value of the specific angular momentum a/M. The solid an dotted curves denote the relativistic and Newtonian disk spectra, respectively.

both effects the investigation of the integrated disk spectrum is treated in two different ways: first, we examine the emergent spectrum of a face on disk as seen for a distant observer without including relativistic effects or Doppler shifts on the locally emitted photon distribution. Relativistic effects only occur due to the relativistic disk structure equations (see section 2.1). The entire spectrum then is simply calculated by integration of the local spectra over the disk surface. In the following we will call this the Newtonian approximation. Second, a fully relativistic calculation of the propagation of photons from the disk to a distant observer is performed, using a program code (Speith et al. 1995) to obtain numerical values of the Cunningham transfer function (Cunningham 1975) for any set of parameters.

The Newtonian disk spectrum for several values of $\dot{M}$ and α is shown in Fig. 8 and 9. The spectral luminosities calculated by summing up local Wien spectra at the corresponding effective temperatures are indicated by dotted lines. The hardness of the spectra and therefore also the amount of soft X–rays is a sensitive function of $\dot{M}$ and a somewhat less sensitive function also of α. In the following, we fix the accretion rate and viscosity parameter at $\dot{M} = 0.3$ and $\alpha = 1/3$, respectively. A comparison of the relativistic and Newtonian face–on disk spectrum for a non–rotating ($a/M = 0$) and maximally rotating ($a/M = 0.998$) black hole is shown in Fig. 10. For low frequencies the emergent spectrum approaches the Newtonian model. The spectrum at higher frequencies is reduced with respect to the Newtonian case especially for a rotating black hole. These photons originate from the inner parts of the disk with high velocities and gravitational fields and therefore are diverted by forward peaking and gravitational focusing. Consequently, an equatorial observer primarily sees blueshifted and focused radiation from the hot inner parts of the disk. In Fig. 11 the observed relativistic spectrum is shown as a function of the inclination angle Θ_0 together with a Newtonian face–on spectrum (dotted line) for a maximally rotating black hole. A

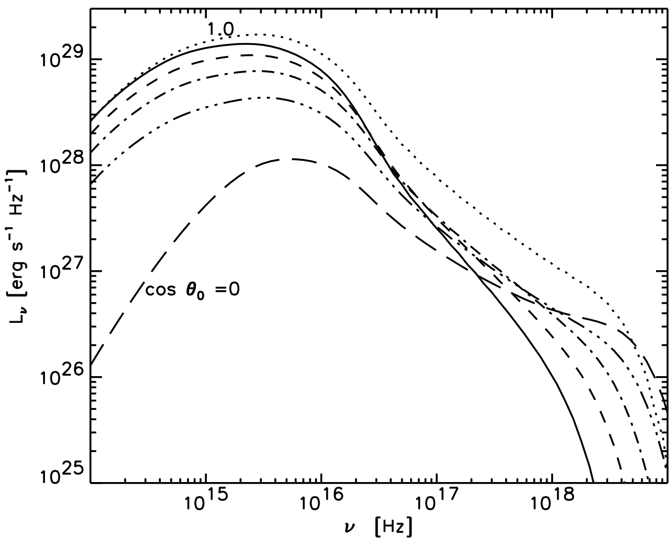

Fig. 11. Entire relativistic disk spectra for different inclination angle $\Theta_0 = 0°, 41°, 60°, 70°$ and $90°$. The model parameters are: $M = 10^8 M_\odot$, $\dot{M} = 0.3$, $\alpha = 1/3$, $a/M = 0.998$. The dotted curve denotes the Newtonian face–on spectrum.

significant fraction of total flux is emitted in the soft and hard X–ray range ($\nu > 2.4 \cdot 10^{16} Hz$) and strongly depends on the position of the observer. For $\Theta_0 = 0°, 41°, 60°, 70°$ and $90°$, this fraction is 36%, 50%, 64%, 78% and 93%, respectively. The fraction of the total flux emitted in the soft X–ray band ($2.4 \cdot 10^{16}\, Hz - 6 \cdot 10^{17}\, Hz$), corresponding to the sensitivity range of the PSPC (position sensitive proportional counter) on the ROSAT X–ray satellite is 32%, 38%, 38%, 33% and 21%, respectively, and therefore is nearly independent of the inclination angle. In order to show the limiting case of our calculations we also included $\cos\Theta_0 = 0$ in Fig. 11. However, for a nearly edge-on observer self–occultation of the inner parts of the disk by the outer parts should be taken into account.

4. Concluding Remarks

We have performed a self–consistent calculation of the vertical structure and emergent spectrum of an accretion disk around a massive Kerr black hole. Full relativistic corrections have been included. The standard α–model leads to diverging temperature profiles in the upper layers of the disk, where the density drops exponentially and viscous heating always overcomes radiative cooling. When we include the radiative cooling of the turbulence elements in the optically thin part of the disk, an equilibrium between turbulent viscous heating and inverse Compton cooling is established. Our calculations are for a fixed central mass $M = 10^8 M_\odot$ but for different $\dot{M}$, α, a/M, and Θ_0. It is found that the mass density is not a monotonically decreasing function of z but shows a strong density inversion in the radiation pressure dominated inner parts of the disk, where the local flux becomes slightly super–Eddington. Moreover, we always obtain a temperature inversion in the upper optically thin layers of the disk with zero gradient in the outermost region. For sufficiently high $\dot{M}$ and α the disk becomes effectively optically thin at small radii and the gas temperature exceeds the equilibrium temperature ($T_{eq} = (U/a_r)^{1/4}$) by a large amount even in the disk midplane. As a result, the local emission spectrum strongly deviates from the Wien spectrum at $T = T_{\rm eff}$. Even in the optically thick case, the local spectra differ from the Wien–spectra at high frequencies, because scattering opacity dominates in the soft X–ray range and there exists a temperature gradient in the vertical direction. Therefore, a significant fraction of the total flux is emitted in the soft X–ray range even for low $\dot{M}$ and α, especially in the maximally rotating case ($a = 0.998$) and for high inclination angles of the observer. For increasing $\dot{M}$, α, a/M, and Θ_0 the calculated spectra become more and more flat, producing quasi power law spectra in the sensitivity range of the ROSAT PSPC, whereas for small values a steep soft X-ray component is established. Thus, the model can in general account for the soft X–ray excess observed in many AGN. We intend to show detailed spectral fits of this model to combined ROSAT and IUE observations for a sample of AGN in a future paper.

Note that we have neglected induced processes and that our opacity description only contains free–free processes for a pure hydrogen atmosphere. Neglecting induced processes means, that we have concentrated on the high energy tail of the resulting spectra. Nevertheless, bound–free absorption and line opacities can significantly contribute to the total opacity especially at low temperatures. Therefore, the spectrum is expected to soften when all relevant opacities are taken into account because of the increasing effective optical depth in this case.

Another important point is the role of convection in our calculations, especially in view of our inverse density profiles. If convective energy transport takes place in the disk, the vertical structure and subsequently the emergent spectrum may be altered considerably. We therefore have done a simplified stability analysis according to the standard mixing length theory (see for example Cox & Giuli 1968), assuming that the convective elements move adiabatically in the disk and that the local gas temperature is given by the equilibrium temperature T_{eq}. In a gas with radiation pressure, the effective buoyancy force is reduced by the radiation pressure gradient and the convective flux then can be expressed in terms of the effective gravitational acceleration g_z^* (equation 31),

$$F_{conv} = \frac{\rho c_P T l_m^2 H_P^{-3/2} \delta^{1/2}}{4\sqrt{2}} \sqrt{g_z^* (\nabla_s - \nabla_e)} \cdot (\nabla_s - \nabla_e) \, , \quad (35)$$

where l_m, $H_P = P/(\rho g_z)$, and c_P are the mixing length, the pressure scale height and the specific heat at constant pressure, respectively, and $\delta = -\partial ln\rho/\partial lnT$. $\nabla_s = (dlnT/dlnP)_s$ and $\nabla_e = (dlnT/dlnP)_e$ are the temperature gradients with respect to pressure for the surroundings and the rising element. Therefore, the disk is unstable for convection if the square root on the right hand side of equation (35) has a positive argument. In the sub–Eddington regime one has $g_z^* > 0$ and the condition for convection to set in is given by the Schwarzschild criterion $(\nabla_s - \nabla_e) > 0$. On the other hand in the super–Eddington regime $g_z^* < 0$, and the condition for convective instability is $(\nabla_s - \nabla_e) < 0$, leading to a convective energy flux in negative z–direction. Our model calculations show that none of both conditions are satisfied and the disk therefore is stable against convection. Since the gas temperature deviates from the equilibrium temperature for an effectively optically thin disk and the convective elements do not move adiabatically in the upper optically thin layers, this simplified stability analysis has to be considered with caution, and a more detailed stability analysis has to be performed in order to clarify the role of convection.

It is well known that an α-disk with a viscosity proportional to the total pressure is radially unstable in the radiation dominated case (Lightman & Eardly 1974). However, this analysis is based on a vertically integrated disk structure. Since our model leads to a strong z-dependence for almost all functions including the viscosity, a detailed 2-dimensional stability analysis would be required for a definite answer concerning the overall stability of our model.

Acknowledgements. T. Dörrer acknowledges the support of DARA through grant 50 OR 90099.

References

Arnaud, K. A. , Branduardi–Raymont, G. , Culhane, J. L. , et al. , 1985, MNRAS, 217, 105

Bechtold, J. , Czerny, B. , Elvis, M. , Fabiano, G. , Green, R. F. , 1987, ApJ, 314, 699

Carson, T. R. , 1988, A& A, 189, 319

Cox, J. P. , & Giuli, R. T. , 1968, in *Principle of Stellar Structure*, Volume 1 (Physical Principles), Gordon & Breach, New York

Cunningham, C. T. , 1975, ApJ, 202, 788
Czerny, C. T. , & Elvis, M. , 1987, ApJ, 321, 305
Felten, J. E. , & Rees, M. J. , 1972, A& A, 17, 226
Hubeny, I. , 1990, ApJ, 351, 632
Karzas, W. J. , & Latter, R. , 1961, ApJS, 6, 167
Kompanaets, A. S. , 1957, Soviet Phys. JETP, 4, 730
Laor, A. , & Netzer, H. , 1989, MNRAS, 238, 897
Laor, A. , Netzer, H. , Piran, T. , 1990, MNRAS, 242, 560
Lightman, A. P. , & Eardley, D. M. , 1974, ApJ, 187, L1
Malkan, M. A. , & Sargent, W. L. W. , 1982, ApJ, 254, 22
Meyer, F. , & Meyer–Hofmeister, E. , 1982, A& A, 106, 34
Milsom, J. A. , Chen, X. , Taam, R. E. , 1994, ApJ, 421, 668
Novikov, I. D. , & Thorne, K. S. , 1973, in *Black Holes*, eds. de Witt, C. & de Witt, B. , Gordon & Breach, New York
Page, D. N. , & Thorne, K. S. , 1974, ApJ, 191, 499
Pounds, K. A. , Nandra, K. , Stewart, G. C. , George, I. M. , Fabian, A. C. , 1990, Nat, 344, 132
Pringle, J. E. , & Rees, M. J. , 1972, A& A, 21,1
Riffert, H. , & Herold, H. , 1995, ApJ, in press
Ross, R. R. , Fabian, A. C. , Mineshige, S. , 1992, MNRAS, 258, 189
Shakura, N. I. , & Sunyaev, R. A. , 1973, A& A, 24, 337
Shields, G. A. , 1978, Nat, 272, 706
Shimura, T. , & Takahara, F. , 1993, ApJ, 419, 78
Shimura, T. , & Takahara, F. , 1995, ApJ, 440, 610
Speith, R. , Riffert, H. , Ruder, H. , 1995, Comp. Phys. Comm. , in press
Thorne, K. S. , 1974, ApJ, 191, 507
Wandel, A. , & Petrosian, V. , 1988, ApJ, 329, L11
Wilkes, B. J. , & Elvis, M. , 1987, ApJ, 323, 243
Turner, T. J. , & Pounds, K. A. , 1989, MNRAS, 240, 833
Yamada, T. T. , Mineshige, S. , Ross, R. R. , Fukue, J. , 1994, PASJ, 46, 553

This article was processed by the author using Springer-Verlag LaTeX A&A style file *L-AA* version 3.